GHGT-11

# CO$_2$ removal at high temperature from multi-component gas stream using porous ceramic membranes infiltrated with molten carbonates

M.-L. Fontaine[a],*, T.A. Peters[a], M.T.P. McCann[a], I. Kumakiri[a], R. Bredesen[a]

*[a]SINTEF Materials and Chemistry, PB 124 Blindern, N-0314 Oslo, Norway*

**Abstract**

This work reports on the investigation of CO$_2$ selective membranes for pre-combustion and post-combustion processes, in which CO$_2$ is extracted from multi-component gas streams at intermediate temperature (400 – 600 °C). The dual-phase membranes developed in this work are designed as a porous oxide ion conducting ceramic matrix, which is infiltrated with a molten carbonate phase. Both ex-situ and in-situ characterization methods were used to study disk shaped and tubular membranes. The gas transport properties of disk-shaped membranes were further investigated under various operating conditions relevant for both post-combustion and pre-combustion applications.

© 2013 The Authors. Published by Elsevier Ltd.
Selection and/or peer-review under responsibility of GHGT

*Keywords: Membrane; CO$_2$ separation; molten carbonate; dual-phase membrane; ionic conductor.*

## 1. Introduction

The primary route for large-scale industrial hydrogen production uses natural gas through a process that involves two equilibrium-limited reactions namely steam reforming and a subsequent water gas shift (WGS) step, to obtain a gas, which is rich in H$_2$ and contains little CO. Hydrogen selective membranes have frequently been studied in membrane reactors for water-gas shift (WGS-MR) and steam reforming (SR-MR) reactions to simultaneously achieve a high methane conversion and production of pure H$_2$. A key feature of this process intensification for pre-combustion decarbonisation is that such a membrane reactor would produce both a high pressure CO$_2$ stream, and high-purity H$_2$ for power generation. Instead

* Corresponding author. Tel.: +47 934 79 555; Fax: +47 2206 7350.
*E-mail address:* Marie-Laure.Fontaine@sintef.no

of applying a membrane to remove $H_2$, one could also apply $CO_2$ selective membranes to remove $CO_2$. Kaggerud et al [1] presented modeling results for both an ideal $H_2$ membrane reactor with infinite selectivity and permeability, and for a $CO_2$ membrane reactor. Their study indicated that $CO_2$ membranes have potential for achieving higher efficiency.

$CO_2$ selective membranes may also be of interest as concentrators of $CO_2$ present in the gas turbine exhaust of a Floating Production Storage and Offloading (FPSO) unit. A FPSO unit is a floating vessel used by offshore industry for hydrocarbon processing and oil storage. The process involves separating liquids and gas to produce oil, store the oil ready for export via tankers, re-inject the associated gas into the reservoir and export the surplus gas to another platform via a sub-sea gas pipeline. Gas turbine exhaust emissions when burning conventional fuels composes primarily of nitrogen (66-72 vol %), $O_2$ (12-18 vol. %), $CO_2$ (1-5 vol. %) and steam (1 to 5 vol. %).

Most research on $CO_2$ selective membranes worldwide focuses on low temperature membrane applications and such membranes have no or limited hydrothermal and chemical stability at temperatures above 300ºC. Microporous membranes with strong $CO_2$ adsorption, show fairly good $CO_2$ selectivity in the presence of a gas with low affinity for the membrane material. For instance, at intermediate temperatures, $CO_2/N_2$ selectivity up to 400ºC and $CO_2/H_2$ selectivity up to 200 ºC are reported for MFI zeolite membranes [2]. At high pressure (10-15 bars) $CO_2$ selectivity has been demonstrated for MFI membranes ($CO_2/N_2$ separation factor ~ 13) with promising $CO_2$ permeance values of $2.7 \cdot 10^{-7}$ mol·m$^{-2}$·s$^{-1}$·Pa$^{-1}$ at 25°C [3, 4]. For ETS-10 membranes $CO_2/N_2$ separation factors between 7–10 have been obtained in the pressure range of 6–22 bar for an equimolar feed mixture [5].

Dual-phase membranes show great potential for high temperature operation. These novel membranes consist of a molten carbonate phase infiltrated in a porous ceramic or metallic support [6-11]. Current investigations on disk-shaped dual-phase membranes are aiming at identifying mechanisms to explain the gas transport properties of these membranes, which depend on materials and processing operations. It has been suggested that the electrical current loop, set up by the transport of $CO_2$ as carbonate ions, is closed by electrical transport in the solid supporting phase. Therefore, oxygen ion conducting materials or metals have been used as supports to facilitate the counter current ionic or electronic transport, respectively. It has been shown that enhanced $CO_2$ flux is obtained in the presence of oxygen on the feed side implying that carbonate ions are the permeating species, and not just dissolved $CO_2$ gas. [6]. To eliminate the need for $O_2$ in the feed stream, the use of a ceramic-like perovskite material, $La_{0.6}Sr_{0.4}Co_{0.8}Fe_{0.2}O_{3-\delta}$ (LSCF) was proposed as the support [9]. This material has been studied extensively as a mixed conductor due to its high electronic and ionic conductivities [12]. Examples of performance for these membranes are $CO_2/Ar$ selectivity above 225 and $CO_2$ permeance in the order of $2-5 \cdot 10^{-8}$ mol·m$^{-1}$·s$^{-1}$·Pa$^{-1}$ at 900 ºC for a porous $La_{0.6}Sr_{0.4}Co_{0.8}Fe_{0.2}O_3$ (LSCF) matrix impregnated with an eutectic molten carbonate mixture ($Li/Na/K_2CO_3$ = 43.5:31.5:25). A dual-phase membrane of $Bi_{1.5}Y_{0.3}Sm_{0.2}O_3$/molten carbonate ($Li/Na/K_2CO_3$ = 43.5/31.5/25) was synthesized by the same group, and used for selective permeation of $CO_2$ at 500 - 650 °C [11]. The $CO_2$ permeation flux for the dual-phase membrane increases with the increase of temperature and reaches a maximum value of $6.6 \cdot 10^{-2}$ mL·cm$^{-2}$·min$^{-1}$ at 650 °C. This equals to a $CO_2$ permeance of $9.7 \cdot 10^{-9}$ mol·m$^{-2}$·s$^{-1}$·Pa$^{-1}$. No value for the $CO_2/Ar$ separation factor was reported.

Results from a theoretical model describing the steady state $CO_2$ flux through a dual-phase membrane suggested that the limiting factor dominating the $CO_2$ flux is the oxide ion conductivity of the porous ceramic matrix [13]. The application of a ceramic oxide with high oxide ion conductivity is thus attracting more attention. A Gadolinium-doped ceria (CGO) / molten carbonate ($Li/Na/K_2CO_3$ = 43.5:31.5:25)

membrane has a $CO_2$ permeance of $3 \cdot 10^{-8}$ mol$\cdot$m$^{-2}\cdot$s$^{-1}\cdot$Pa$^{-1}$ at 850 °C in an equimolar feed of $CO_2$/He [14]. The separation factor obtained in this study, however, was relatively low, $< 20$, based on the reported helium permeability/leakage. Though encouraging, these results point out the need for further investigation of these novel membranes and their transport properties.

In this work, we present a manufacturing protocol developed for producing disk-shaped membranes as well as thin film supported tubular membranes using a melt impregnation method. A variety of membranes are produced using ceria-based ceramic oxides and various binary and ternary mixtures of carbonates. The membranes were thoroughly characterized by ex-situ and in-situ analyses.. Membrane performance was evaluated by applying different operating conditions representative for both pre- and post-combustion membrane operation, including various partial pressures of $CO_2$ and $O_2$ in the feed gas mixtures and use of steam.

## 2. Experimental

### 2.1. Dual-phase membrane preparation

The flowchart showing the method developed for the preparation of disk-shaped and tubular dual-phase membranes is given in Figure 1. For the former membranes, porous disks of $CeO_2$ and Sm/Gd doped $CeO_2$ are prepared from commercially available $CeO_2$ powder (Aldrich, sub-micron grain size) and $Ce_{0.85}X_{0.15}O_{2-\delta}$ powder (X= Gd or Sm – Aldrich, nano-sized grain). Chitosan (Yuhauan Ocean Biochemical Co.) is used as pyrolyzable filler to control the porosity of the ceramics after annealing. The ceramic-filler powder mixtures are pressed in a steel die of 20 mm diameter. The produced green pellets are annealed in air. The temperature is adjusted to obtain a desirable trade-off between mechanical strength and open porosity of these supports. The annealed disks are dipped in a molten carbonates melt. The melt is obtained by mixing and annealing in air at 600 °C binary and ternary mixtures of Li$^+$, Na$^+$ and K$^+$ carbonate salts. The samples are then quenched to room temperature. Both sides of the membranes are polished to remove the excess of carbonate layers from the surfaces of the samples. The membranes are referred to as Li-K-Na/ $CeO_2$ for ceria infiltrated with the Li$^+$, Na$^+$ and K$^+$ eutectic mixture and Li-K-Na/ GDC (or SDC), for Gd (or Sm) doped ceria infiltrated with Li$^+$, Na$^+$ and K$^+$ eutectic mixture. Commercially available porous alumina tubes with graded porosity are used for the fabrication of tubular supports. They are dip-coated in a suspension of $CeO_2$ and Sm/Gd doped $CeO_2$ prepared by mixing the powders in isopropanol with a dispersant and polyvinyl butyral binder. The coated tubes are then annealed in air at 1200 °C for consolidation of the ceria-based layer. The coated tubes are then dip-coated in molten carbonates and then slowly cooled down to room temperature. A second annealing step at 600 °C is carried out for further infiltration of the molten phase in the ceria layer.
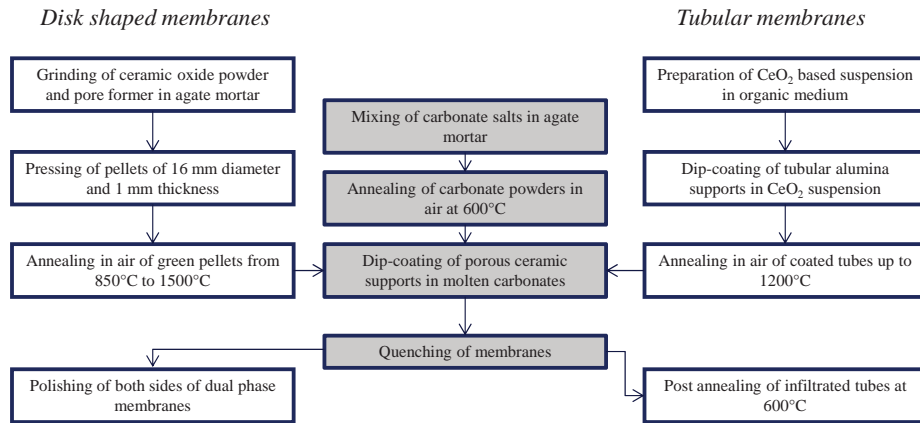
*Disk shaped membranes*                                                      *Tubular membranes*



Fig. 1. Flowchart of the procedure developed for preparing disk-shaped and tubular dual-phase membranes

## 2.2. Characterisation

### 2.2.1. Ex-situ analyses
X-ray diffraction (XRD) patterns of powders and membranes before and after testing were collected with a Siemens D710 diffractometer. Microstructural investigation of samples was performed with a JEOL JSM-5900LV SEM microscope equipped with electron dispersive spectroscopy (EDS) detector for chemical composition analysis.

### 2.2.2. In-situ analyses
In order to observe the melting behaviour of the carbonate phase, the composite membranes were investigated upon annealing with an environmental scanning electron microscope (ESEM FEI Quanta 200 F). The SEM is equipped with a field emission gun with an acceleration voltage between 200 V – 30 kV and a high temperature furnace enabling observation up to 1500 °C. A ceramic gaseous backscattered diffraction detector is used in this work. The samples are placed in a Pt crucible and heated in 200 Pa water vapour at a rate of 50 °C/min from room temperature to 400 °C followed by a rate of 20 °C/min from 400 °C to 500 °C, and finally a rate of 10 °C/min from 500 to 600 °C. A HSM-ODHT heating microscope combined with an optical dilatometer was also used to observe the wetting behaviour of dual-phase membranes upon annealing in air up to 650 °C with a heating rate of 10 °C/min.

### 2.2.3. Permeation measurements
Flux measurements were performed in a Probostat$^{TM}$ cell. Automated mass flow controllers (Bronkhorst High-Tech) were used to control the gas supply to the feed and permeate sides of the membranes. Silver paste was used to seal the membranes. The membranes were firstly heated in a mixture of air and helium up to 400 °C. $CO_2$ (99.995%) was then introduced on the feed side of the membranes and various gas mixtures were then applied to both the feed and permeate sides of the membranes. In all experiments, He was kept in the feed side of the membranes as a probing gas to check for potential leakage during testing. The total flow rate applied at the feed side was equal to 50 NmL·min$^{-1}$. A sweep flow of 25 NmL·min$^{-1}$ of Ar (99.999%) was applied at the permeate side. Both pressures of the feed and permeate side of the

membranes were kept at atmospheric pressure in all experiments. The $CO_2$ and $O_2$ fluxes were calculated from the measured concentrations in the permeate using the calibrated flow of Ar sweep gas. The permeate composition was monitored by a gas chromatograph (Varian Inc., CP-4900) equipped with a thermal conductivity detector (TCD).

## 3. Results and discussion

### 3.1. Structure and microstructure of membranes

#### 3.1.1. Disk-shaped membranes

The procedure for the preparation of the dual-phase membranes was firstly established on disk-shaped membranes using both sub-micron sized and nano-sized ceria powders to prepare porous disks with various pore size. For this purpose, sub-micron sized $CeO_2$ powder was mixed with chitosan filler consisting of acicular grains with size ranging from 2 to 20 microns (Figure 2a). Annealing of these disks in air at 1500 °C resulted in mechanically strong ceramics with a pore volume of about 35 vol. % (Figure 2b) and large grains between 2 and 5 microns in size. The disks contain pores of about 2 to 5 microns from partial sintering of $CeO_2$ grains and large transversal pores up to 20 microns resulting from the burnout of chitosan granules.
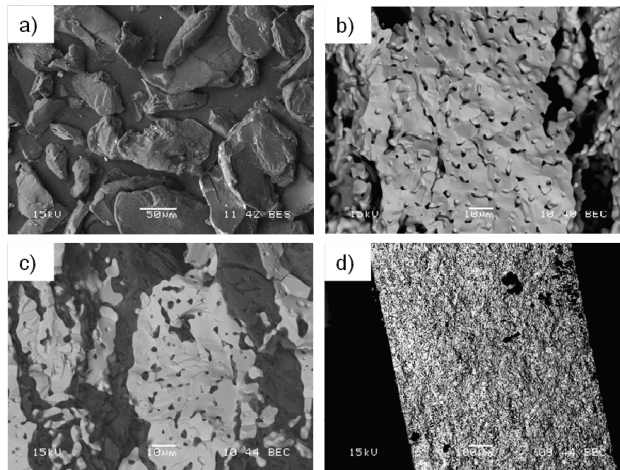


Fig. 2. SEM micrographs of a) chitosan granules; cross-section views of b) $CeO_2$ porous disk before infiltration; c) and d) $CeO_2$ porous disk after infiltration in Li/K melt $(Li_{0.62}K_{0.38})_2CO_3$ with two different magnifications

Melt impregnation of the porous disks yielded complete infiltration of the porous ceria support, as shown in Figures 2c and 2d for Li-K/$CeO_2$ membrane. The membranes exhibit two interconnected networks of a carbonate phase and a ceramic phase. Nano-sized doped $CeO_2$ powder was also used to produce porous disks with equivalent pore volume (35 vol. %) and small grains below 500 nm size (Figure 3a) after annealing at 850 °C. The consolidated disks have small pores below 500 nm size. After melt infiltration, the resulting Li-K/GDC membranes have a fine microstructure with small ceramic grains and pores filled with carbonates (Figure 3b). XRD analysis at room temperature revealed that the crystalline carbonate phase has a pattern indexed with the JCPDS file of $LiKCO_3$ carbonate phase.
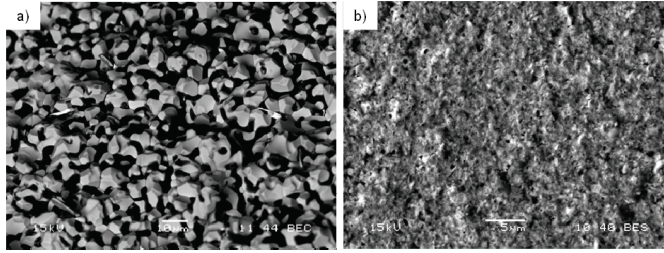
Fig. 3. SEM micrographs in cross-section view of a) fractured Li-K/CeO$_2$ membrane and b) fractured Li-K/GDC membrane

### 3.1.2. Thin film tubular membranes

Melt infiltration of ceria-coated alumina tubes resulted in the deposition of a carbonate layer on the surface of the porous ceria layer, as shown in Figure 4. There was poor infiltration of the carbonate phase in the ceria layer during the first dipping step. In order to obtain a more uniform composite Li-K/CeO$_2$ membrane, it was necessary to anneal the membranes in air at 600 °C for 30 min to allow the melt to infiltrate the ceria layer, as shown in Figure 5.

Gas permeation tests at room temperature were carried out after each fabrication step to quality-assess the procedure. The ceria-coated alumina tube has a permeance of $5.0 \cdot 10^{-5}$ mol·m$^{-2}$·s$^{-1}$·Pa$^{-1}$ which is close to the one measured for the bare alumina tube of $2.0 \cdot 10^{-4}$ mol·m$^{-2}$·s$^{-1}$·Pa$^{-1}$. After post-annealing, the membrane with the solid carbonate phase in the porous support has a significantly lower permeance of $5 \cdot 10^{-8}$ mol·m$^{-2}$·s$^{-1}$·Pa$^{-1}$. These results indicate that the ceria layer is porous with little effect on gas flow through the support. Besides, the molten phase has fairly well infiltrated the pores of the ceria layer.
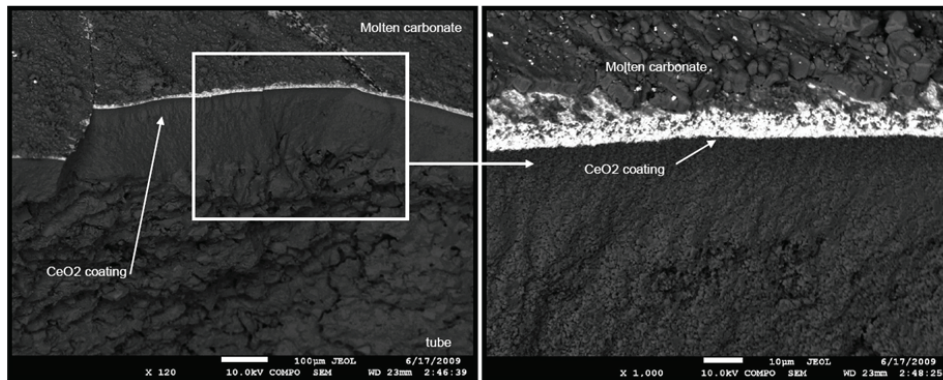


Fig. 4. Cross-section view of fractured tubular membrane showing the graded porosity in the alumina support tube, the porous ceria layer (in white) and a layer of carbonate poorly infiltrated in the ceria layer (in grey)
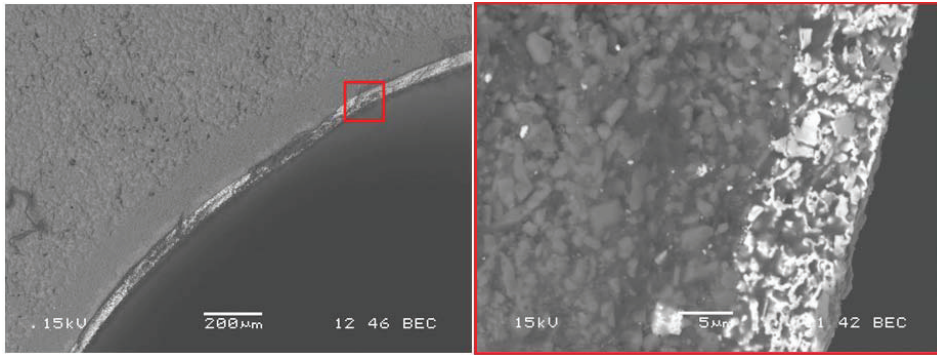
Fig. 5. Cross-section view of polished tubular membrane showing the graded porosity in the alumina support tube, and the porous ceria layer (in white) infiltrated with carbonate (in grey)

### 3.2. In-situ observations of composite membranes

Li-K/CeO$_2$ membranes were observed by FEG-SEM upon annealing up to 600 °C. SEM micrographs were registered at various temperatures, as illustrated in Figure 6 for selected pictures. From these observations, it was found that the microstructure of the dual-phase membrane does not evolve from room temperature up to 400 °C. Above this temperature, pinholes initially present in the solid carbonate phase disappear and the carbonate surface seems smoother, indicating surface melting between T = 450 °C and T = 500 °C (Figures 6.4 and 6.5). Further increase in temperature yields bulk melting of the carbonate phase and its infiltration in the porous ceramic support (see micrograph 6.9).
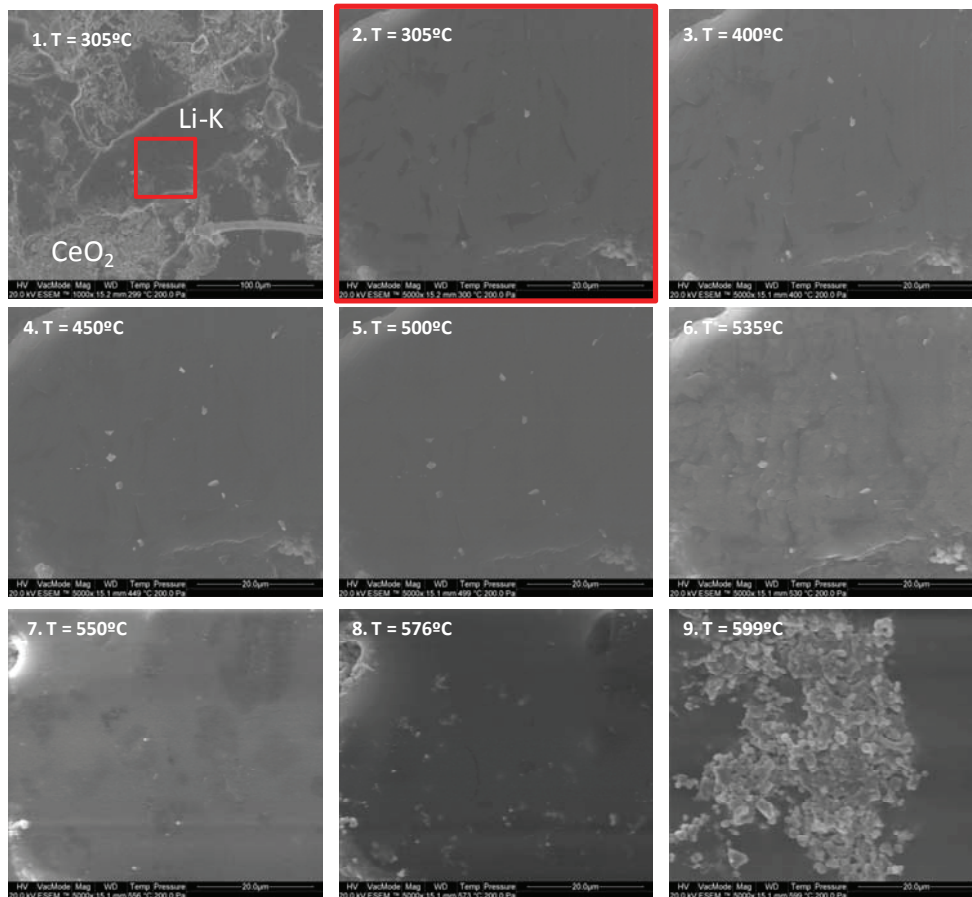
Fig. 6. SEM micrographs taken upon annealing a Li-K/CeO$_2$ membrane. Micrograph 1 is taken with lower magnification and is used as reference. Micrographs 2-8 are taken with higher magnification and only the carbonate phase is visible. In micrograph 9, both ceramic and carbonate phases are visible

The membranes were also observed with a combined heating microscope and dilatometer upon annealing in air. As shown in Figure 7, the shape of the membrane evolves between 400 °C and 450 °C: a liquid is expanding out of the ceramic matrix and shows a fairly good wettability to the ceramic oxide as indicated by the low contact angle (see picture at T = 425 °C). At 479 °C, the carbonate phase has melted and is wetting both the ceramic oxide and the alumina plate used as a support for the experiment.

Fig. 7. Pictures taken by optical dilatometer upon annealing in air of Li-K/CeO$_2$ membranes. Circles highlight changes occurring during annealing. Notice that the excess of Li/K carbonate after dip-coating of the porous disk has delaminated from the surface of the ceramic upon annealing from room temperature to 90 °C

### 3.3. Performance of membranes

CO$_2$ flux and CO$_2$/He selectivity of a 1 mm thick Li-K-Na/SDC disk-shaped membrane are illustrated in Figure 8 using a feed gas mixture containing CO$_2$:O$_2$:He = 60:20:20 vol.% during ramping from 525 °C to 700 °C. It can be seen that the CO$_2$ flux increases from around 0.03 to 0.15 mL·cm$^{-2}$·min$^{-1}$, with an increased CO$_2$/He separation factor from 150 to 1074 at 700 °C. The calculated activation energy for the flux equals to 65.7 kJ·mol$^{-1}$. For comparison, Anderson and Lin report an activation energy for Li-K-Na/LSCF-disk-shaped membrane of about 87 kJ·mol$^{-1}$, while a value of 113 kJ·mol$^{-1}$ was reported by the same group for a Li-Na-K / BYS membrane [11]. These values are obtained for feed gas mixtures with no O$_2$ present.
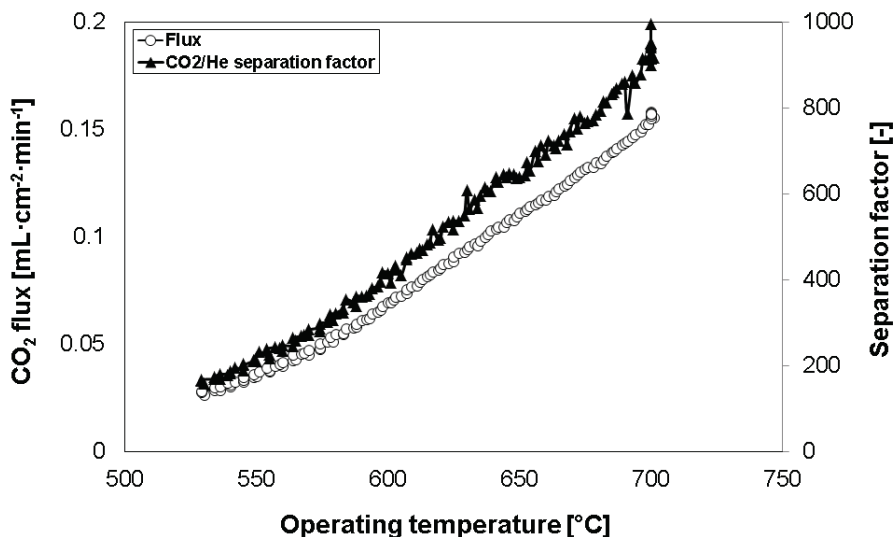
Fig. 8. Effect of operating temperature on $CO_2$ permeation properties of a 1mm thick Li-Na-K/SDC disk-shaped membrane ($Li/Na/K_2CO_3 = 43.5:31.5:25$). Feed gas mixture contains $CO_2:O_2:He = 60:20:20$ and argon is applied as sweep

Effects of $O_2$ and steam concentrations on both sides of the membranes are currently investigated and will be published in a forthcoming paper.

### 4. Conclusions

This work reports on the successful preparation of $CO_2$ selective disk-shaped membranes and thin film tubular membranes. The former are made of a porous disk of oxide ion conductor embedded in a molten carbonate phase. The latter consist of a composite layer of carbonate-oxide and oxide ion conductor deposited on commercially available porous alumina supports. Melt impregnation of the consolidated ceramic matrix is used to produce the dual-phase membranes. Flux permeation measurements of Li-K-Na/SDC membranes confirmed that the membranes exhibit high selectivity of $CO_2$ over He and fairly high permeance at temperatures above 525 °C.

### Acknowledgements

# References

[1]    Kaggerud K, Gjerset M, Mejdell T, Kumakiri I, Bolland A, Bredesen R. Power production with $CO_2$ management-integration of high temperature $CO_2$ selective membranes in power cycles. *Greenhouse Gas Control Technologies* 2005;**7**:1857-60.

[2]    Kumakiri I, Lecerf N, Bredesen R. Microporous inorganic membranes for $CO_2$ separation. *Transactions of the Materials Research Society of Japan* 2004;**29**:3271-4.

[3]    Sebastian V, Kumakiri I, Bredesen R, Menendez M. Zeolite membrane for $CO_2$ removal: Operating at high pressure. *Journal of Membrane Science* 2007;**292**:92-7.

[4]    Sebastian V, Kumakiri I, Bredesen R, Menendez M. Zeolite membrane for $CO_2$ removal: operating at high pressure. *Desalination* 2006;**199**:464-5.

[5]    Tiscornia I, Kumakiri I, Bredesen R, Tellez C, Coronas J. Microporous titanosilicate ETS-10 membrane for high pressure $CO_2$ separation. *Separation and Purification Technology* 2010;**73**:8-12.

[6]    Chung SJ, Park JH, Li D, Ida JI, Kumakiri I, Lin JYS. Dual-phase metal-carbonate membrane for high-temperature carbon dioxide separation. *Ind Eng Chem Res* 2005;**44**:7999-8006.

[7]    Kawamura H, Yamaguchi T, Nair BN, Nakagawa K, Nakao S. Dual-ion conducting lithium zirconate-based membranes for high temperature $CO_2$ separation. *Journal of Chemical Engineering of Japan* 2005;**38**:322-8.

[8]    Yamaguchi T, Niitsuma T, Nair BN, Nakagawa K. Lithium silicate based membranes for high temperature $CO_2$ separation. *Journal of Membrane Science* 2007;**294**:16-21.

[9]    Anderson M, Lin YS. Carbonate-ceramic dual-phase membrane for carbon dioxide separation. *Journal of Membrane Science* 2010;**357**:122-9.

[10]   Rui Z, Anderson M, Lin YS, Li Y. Modeling and analysis of carbon dioxide permeation through ceramic-carbonate dual-phase membranes. *Journal of Membrane Science* 2009;**345**:110-8.

[11]   Li Y, Rui Z, Xia C, Anderson M, Lin YS. Performance of ionic-conducting ceramic/carbonate composite material as solid oxide fuel cell electrolyte and $CO_2$ permeation membrane. *Catalysis Today* 2009;**148**:303-9.

[12]   Teraoka Y, Zhang HM, Okamoto K, Yamazoe N. Mixed Ionic-Electronic Conductivity of $La_{1-x}Sr_xCo_{1-y}Fe_yO_{3-delta}$ Perovskite-Type Oxides. *Materials Research Bulletin* 1988;**23**:51-8.

[13]   Wade JL, Lackner KS, West AC. Transport model for a high temperature, mixed conducting $CO_2$ separation membrane. *Solid State Ionics* 2007;**178**:1530-40.

[14]   Wade JL, Lee C, West AC, Lackner KS. Composite electrolyte membranes for high temperature $CO_2$ separation. *Journal of Membrane Science* 2011;**369**:20-9.